

# Lawrence Berkeley National Laboratory

## Recent Work

### Title

CATALYTIC SYNTHESIS OF HYDRO-CARBONS OVER GROUP VIII METALS. A DISCUSSION OF THE REACTION MECHANISM

### Permalink

<https://escholarship.org/uc/item/89540932>

### Author

Bell, A.T.

### Publication Date

1980-09-01



# Lawrence Berkeley Laboratory

UNIVERSITY OF CALIFORNIA

## Materials & Molecular Research Division

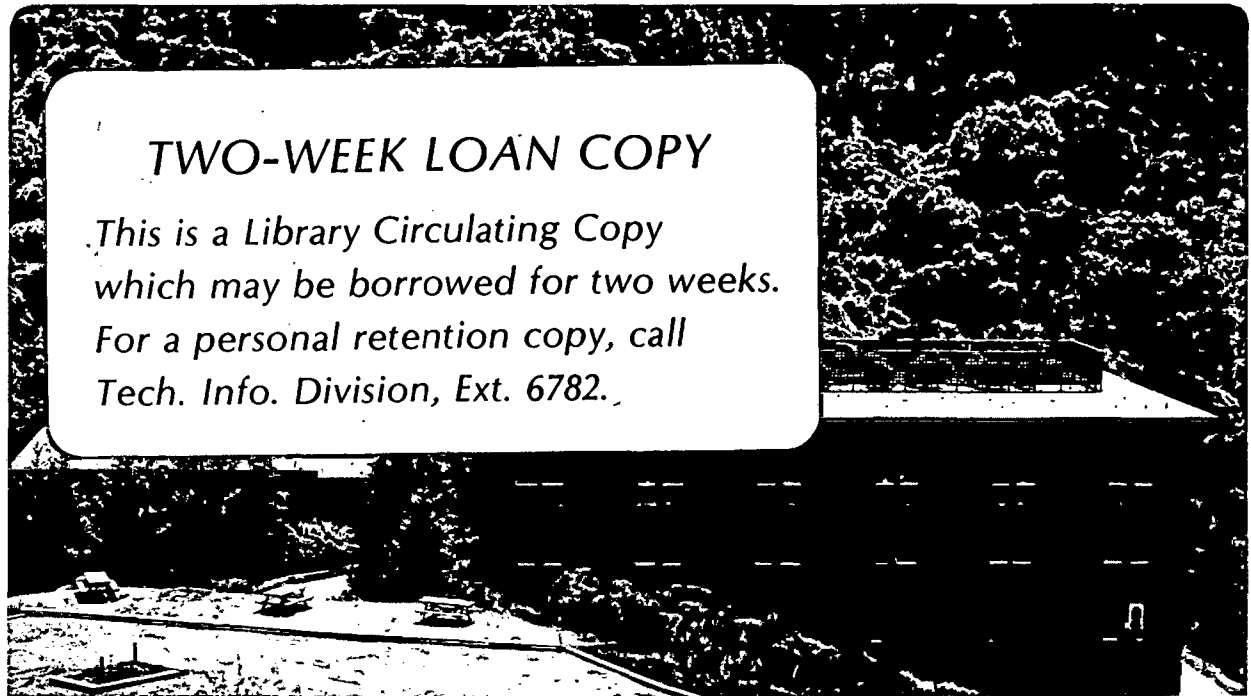
To be published in the Proceedings of the Symposium of Catalysis and Surface Science, "Catalysis Review Science and Engineering," Marcel Dekker, Inc. N.Y., Vol. 23, Nos. 1 & 2, 1981

CATALYTIC SYNTHESIS OF HYDROCARBONS OVER GROUP VIII METALS. A DISCUSSION OF THE REACTION MECHANISM

Alexis T. Bell

September 1980

RECEIVED  
LAWRENCE  
BERKELEY LABORATORY  
NOV 20 1980  
LIBRARY AND  
DOCUMENTS SECTION



**TWO-WEEK LOAN COPY**  
*This is a Library Circulating Copy which may be borrowed for two weeks. For a personal retention copy, call Tech. Info. Division, Ext. 6782.*

LBL-11339 c.2

## DISCLAIMER

This document was prepared as an account of work sponsored by the United States Government. While this document is believed to contain correct information, neither the United States Government nor any agency thereof, nor the Regents of the University of California, nor any of their employees, makes any warranty, express or implied, or assumes any legal responsibility for the accuracy, completeness, or usefulness of any information, apparatus, product, or process disclosed, or represents that its use would not infringe privately owned rights. Reference herein to any specific commercial product, process, or service by its trade name, trademark, manufacturer, or otherwise, does not necessarily constitute or imply its endorsement, recommendation, or favoring by the United States Government or any agency thereof, or the Regents of the University of California. The views and opinions of authors expressed herein do not necessarily state or reflect those of the United States Government or any agency thereof or the Regents of the University of California.

Catalytic Synthesis of Hydrocarbons  
Over Group VIII Metals.  
A Discussion of the Reaction Mechanism

by

Alexis T. Bell

Materials and Molecular Research Division  
Lawrence Berkeley Laboratory

and

Department of Chemical Engineering  
University of California, Berkeley, California 94720

Submitted to  
Catalysis Reviews  
Science and Engineering

This manuscript was reproduced with originals provided by  
the author.

## INTRODUCTION

A broad range of hydrocarbons and oxygenated products can be synthesized catalytically from CO and H<sub>2</sub>, produced by the gasification of coal. Since the earliest examples of such chemistry were reported by Fischer and Tropsch (1,2) in 1926, the nonselective generation of organic compounds via the hydrogenation of CO has become known as Fischer-Tropsch synthesis. In the intervening fifty-four years many efforts have been made to identify the mechanism by which reactants are converted to products. These studies have been motivated in large measure by the desire to understand how catalyst composition and reaction conditions govern the distribution of products formed. A brief review of the mechanistic hypotheses developed prior to 1970 will be presented here to serve as background for a discussion of more recent ideas. Details concerning the earlier studies can be found in a number of reviews (3-15) published previously.

The earliest ideas concerning CO hydrogenation were proposed by Fischer and Tropsch in 1926 (2). They hypothesized that CO reacts with the metal of the catalyst to form a bulk carbide, which subsequently undergoes hydrogenation to form methylene groups. These species were assumed to polymerize to form hydrocarbon chains that then desorb from the surface as saturated and unsaturated hydrocarbons. A more detailed statement of what came to be known as the carbide theory was later proposed by Craxford and Rideal (16-18). These authors suggested that only surface carbides need be considered and that the methylene groups, formed by hydrogenation of the carbide react to produce adsorbed macromolecules. The formation of low molecular weight olefins and paraffins was assumed to occur via the hydrocracking of these macromolecules.

Both versions of the carbide theory were subjected to criticism during the late nineteen forties by Emmett et al. (19-21). Based on the results of thermodynamic,  $^{14}\text{C}$  tracer, and synthesis studies performed with iron and cobalt catalysts, it was concluded that bulk phase carbide participates in the synthesis to a negligible extent. It was also noted that hydrogenation of surface carbides, formed by precarbiding a catalyst with CO, could account for only a small fraction (10-20%) of the hydrocarbons formed during steady state synthesis. Allowance was made, however, for the possibility that chemisorbed carbon atoms might still be considered as intermediates.

Several alternatives were proposed to replace the early carbide theories. Eidus (22) suggested that molecularly adsorbed CO was hydrogenated to form a hydroxycarbene or enol,  $\text{M}=\text{CH}(\text{OH})$ , which then underwent further hydrogenation to produce a methylene group. The growth of hydrocarbon chains was envisioned to occur by polymerization of these latter species. The formation of enol intermediates was also proposed by Storch et al. (3) but it was suggested that chain growth takes place by the condensation of enol groups with the concurrent elimination of water. Yet another mechanism for chain growth was proposed by Pichler and Buffleb (23) and later by Sternberg and Wender (24). In this instance, molecular CO was postulated to insert into the metal-carbon bond of an adsorbed alkyl species. Hydrogenation of the resulting acyl group was assumed to produce water and a new alkyl group containing an additional methylene unit. Pichler et al. (9) proposed that the chain is initiated by methyl groups formed by stepwise hydrogenation of molecularly adsorbed CO. Ponc (13), on the other hand, suggested that the methyl groups might be formed by hydrogenation of surface carbon atoms, created by the dissociation of CO.

The renewed interest in Fischer-Tropsch synthesis experienced during the past decade has motivated a careful reexamination of the previously proposed mechanisms and brought forward a number of new results. The most significant outcome of these recent investigations has been the suggestion that nonoxygenated, rather than oxygenated, intermediates play a dominant role in the synthesis of hydrocarbons from CO and H<sub>2</sub>. Moreover, results obtained from the fields of surface science, organometallic chemistry, and catalysis strongly support the hypothesis that hydrocarbon synthesis is initiated by the dissociation of CO and that the carbon atoms thus produced are hydrogenated to form adsorbed methylene and methyl groups. The latter species may be considered as precursors to methane as well as centers for hydrocarbon chain growth; a process which is postulated to begin by the insertion of a methylene group into the metal-carbon bond of a methyl group. The function of this review will be to summarize the evidence leading to this view of Fischer-Tropsch synthesis and to illustrate its implications for the synthesis of hydrocarbons. In addition, brief discussions will be presented concerning the participation of olefins in secondary reactions, which serve to alter the final distribution of products, and the relationship of the mechanism of hydrocarbon synthesis to that for the synthesis of oxygenated products.

#### ASSOCIATIVE AND DISSOCIATIVE CHEMISORPTION OF CARBON MONOXIDE

Extensive evidence from UPS and IR studies indicates that with few exceptions CO is bonded perpendicularly to the surface of transition metals, through the carbon end of the molecule (25-31). The metal-carbon bond may be formed with either a single metal atom giving rise to linear bonding or may be shared between two or more metal atoms to produce bridge or multiple bonding. Theoretical calculations support the

configurations proposed on the basis of experimental observations and indicate that the metal-carbon bond is comprised of two components (32-34). The first arises from an overlap of the occupied  $5\sigma$  orbital of CO and unoccupied metal orbitals. This results in the donation of electrons from the molecule to the metal. The second component of the metal-carbon bond is formed by backdonation of electrons from occupied metal orbitals to the unoccupied  $2\pi^*$  orbitals of CO. By contrast, the  $4\sigma$  and  $1\pi$  orbitals are thought not to participate appreciably in bond formation with the surface (35,36). Since the  $5\sigma$  orbital in gaseous CO is essentially non-bonding with respect to the C-O bond (36,37), the donation of electrons from this orbital is not expected to affect strongly the strength of the C-O bond in chemisorbed CO. The  $2\pi^*$  orbitals, on the other hand, are anti-bonding (37) with respect to the C-O bond and backdonation into these orbitals leads to a weakening of the bond. Thus, the net effect of donation and backdonation is the formation of a M-C bond and the concurrent weakening of the C-O bond.

Dissociative chemisorption of CO is also known to occur on the surface of many transition metals and most likely proceeds via the molecularly adsorbed state. Figure 1 identifies those metals on which dissociative as opposed to associative adsorption is preferred at room temperature. As may be seen, the tendency for dissociative adsorption increases moving from right to left across a row and upwards in each group. Brodén et al. (26) have noted that this trend parallels the increase in the separation between the  $1\pi$  and  $4\sigma$  states of molecularly adsorbed CO observed by UPS. Since the value of  $\Delta(1\pi-4\sigma)$  is 2.75 eV for gas phase CO and increases with elongation of the C-O bond, it is concluded that stretching of the C-O bond is a prerequisite for dissociation. A similar conclusion may also be drawn from infrared



observations, which show that the vibrational frequency of the C-O bond decreases proceeding from right to left across a row. Since the vibrational frequency reflects the force constant for vibration, and this parameter can in turn be related to the bond length and bond order, it can be demonstrated that a decrease in the CO vibrational frequency coincides with a decrease in the bond order (38,39).

While metals to the right of the dividing line in Fig. 1 will adsorb CO associatively at room temperature, dissociative adsorption can occur at higher temperatures. The energetics involved in converting from the associative to the dissociative state are illustrated in Fig. 2 for the cases of Ni and Ru (40). It is apparent that while the heats of adsorption for molecularly adsorbed CO on Ni and Ru are comparable, the sum of the binding energies for adsorbed carbon and oxygen atoms are not. As a consequence of this fact, the dissociation of associatively adsorbed CO is exothermic on Ni and endothermic on Ru.

The structure of the transition state for CO dissociation is not known but may be assumed to involve simultaneous interactions of both the carbon and oxygen portions of the molecule with two or more sites on the catalyst. A possible prototype for such bonding is found in the structure of  $[\text{Fe}_4(\text{CO})_{13}\text{H}]^-$  (41), where one of the carbonyl ligands is bonded through both the carbon and oxygen atoms to two of the iron atoms associated with the cluster framework. Since the initial bonding of chemisorbed CO is through the carbon end of the molecule, interaction of the surface with the oxygen end of the molecule very likely proceeds via vibrational deformation of the M-C-O bond angle; a process which occurs more readily for multiply-bonded than linearly-bonded CO (42).

The preferential dissociation of multiply bonded CO and the need for an ensemble of metal sites to effect dissociation are further supported by studies reported by Ponec et al. (43, 44) on Ni/Cu alloys. Over a portion of the composition range these metals form miscible alloys in which nickel is active for CO dissociation while copper is not. The addition of copper to nickel reduces the concentration of multiply bonded CO and the extent of CO disproportionation, but does not significantly affect the rate coefficient for disproportionation. Since it is known that the electronic properties of nickel vary only marginally by alloying with copper (45), it was concluded that the main effect of copper addition was to dilute the active nickel in an inactive matrix of copper. Such dilution diminishes the concentration and size of the nickel clusters present in the alloy and hence the availability of ensembles of nickel sites for CO dissociation.

The activation energy for CO dissociation on transition metals has not been measured experimentally, but theoretical estimates have been reported (46,47). Based on CNDO calculations, Robertson and Wilmsen (46) obtained a value of 27 kcal/mole for the dissociation of a CO molecule initially attached in a vertical position to two Ni atoms. More recently, Miyazaki (47) has used the Bond Energy Bond Order model to estimate the interaction energy between a CO molecule and each of the transition metals. Values of the activation energy for dissociation from the molecular state determined from the plots given by Miyazaki are indicated in Fig. 1. As can be seen, the activation energy is predicted to decrease as one proceeds from right to left across a row, paralleling the decreasing bond order of the C-O bond.

FORMATION AND REACTION OF  
NONOXYGENATED INTERMEDIATES

The dissociative chemisorption of CO at elevated temperatures is usually accompanied by the release of oxygen in the form of CO<sub>2</sub>. The overall process is known as CO disproportionation and leads to the accumulation of carbon on the catalyst surface. Auger electron spectroscopy studies conducted with nickel and ruthenium surfaces (48-50) have shown that isolated carbon atoms deposited at temperatures below about 300°C exhibit a fine structure comparable to that of metal carbides. This type of carbon has been referred to as carbidic. Carbon deposition at higher temperatures, however, is characterized as graphitic. Once deposited, carbidic carbon can be converted to the graphitic form by heating, but this transformation is irreversible (51).

In a seminal study Wentrcek et al. (52) observed that hydrogenation of the carbon deposited by CO disproportionation readily produced methane. Subsequent studies (43, 53-55) confirmed this result and showed that higher molecular weight hydrocarbons can be formed in addition to methane. Auger spectra taken of the surface of catalysts in the form of single crystals and foils, reveal further that carbidic carbon reacts much more rapidly than graphitic carbon. While the details of the hydrogenation process are not fully understood, it seems reasonable to propose that the first stages involve the formation of CH, CH<sub>2</sub>, and CH<sub>3</sub> groups by the stepwise addition of atomic hydrogen to single carbon atoms. The existence of such species as ligands in both mono- and poly-nuclear transition metal complexes is well established (56) and the presence of CH, and possibly CH<sub>2</sub> groups, on a Ni (111) surface has been reported recently (57,58).

The stereochemistry and reactivity of carbon atoms and CH<sub>x</sub> (x=1-3) species associated with cluster complexes have been investigated in a few cases (56). Since these structures can be viewed as models for the surface of a transition metal, a brief summary of selected results will be presented.

Studies by Muetterties et al. (56,59,60) strongly suggest that the reactivity of carbidic carbon atoms increases as the coordination number of the carbon atom decreases. Thus, the  $\mu_5$ -C carbide atom in  $\text{Fe}_5\text{C}(\text{CO})_{15}$  is non-reactive up to  $80^\circ\text{C}$  where this cluster decomposes (56). By contrast, oxidation of  $\text{Fe}_4\text{C}(\text{CO})_{12}^{2-}$  with  $\text{Ag}^+$  in the presence of  $\text{H}_2$  yields  $\text{HFe}_4(\text{CH})(\text{CO})_{12}$  indicating a direct hydrogenation of the cluster  $\mu_4$ -C carbide carbon atom at  $25^\circ\text{C}$  (59,60). Structural characterization of the methylidyne containing species shows that the CH unit is bonded through both the C and H atoms. Moreover, NMR studies indicate a fast exchange of hydrogen between the hydridic site and the CH site.

The interrelationships between CH,  $\text{CH}_2$ , and  $\text{CH}_3$  species have been studied by Shapley et al. (61-63). Their work has shown that the preparation of  $\text{Os}_3(\text{CO})_{10}\text{CH}_4$  leads to an equilibrium mixture containing the methyl species  $\text{H}(\text{CH}_3)\text{Os}_3(\text{CO})_{10}$  and the  $\mu_2$ -methylene species  $\text{H}_2(\text{CH}_2)\text{Os}_3(\text{CO})_{10}$  (Fig. 6) and that a methylene structure  $\text{H}_3\text{Os}_3(\text{CO})_9(\text{CH})$  can be produced upon extended heating of a nitrogen flushed solution of the methyl and methylene structures. The  $\mu_2$ -bonding of the methylene group, is characteristic of such ligands and is observed in systems involving Fe and Ru (64,65) as well. Attention is also drawn to the asymmetric bridge-bonding of the methyl group, since it may be representative of the transition state structure for methylene-methyl interconversion. Finally, it is noted that the hydrogen atoms associated with the methyl and methylene groups are labile and in rapid exchange with the hydride ligands; a conclusion which is drawn from NMR studies with partially deuterated analogs of  $\text{H}(\text{CH}_3)\text{Os}_3(\text{CO})_{10}$  and  $\text{H}_2(\text{CH}_2)\text{Os}_3(\text{CO})_{10}$ .

Identification of the processes involved in the formation of hydrocarbons containing two or more carbon atoms is central to understanding the chemistry which controls the distribution of hydrocarbons produced by Fischer-Tropsch synthesis. With this aim in mind, recent investigators have attempted to establish the extent to which surface carbon and adsorbed CO participate in the formation of  $C_{2+}$  hydrocarbons. Studies by Rabo et al. (53) have shown that hydrogenation of surface carbon deposited on nickel, cobalt, and ruthenium catalysts via CO disproportionation leads to the appearance of ethane, propane, and butane, in addition to methane. The formation of hydrocarbons is very rapid and quantitative consumption of the carbon can be achieved at room temperature. By contrast, chemisorbed CO was found to be totally unreactive at this temperature. Similar observations were reported by Low and Bell (54) for the formation of ethane over a ruthenium catalyst.

In studies conducted by Ekerdt and Bell (66) it was shown that under reaction conditions the surface of a ruthenium catalyst is largely covered by CO and maintains a carbon reservoir of up to several monolayers of the metal. Passage of hydrogen over the catalyst following steady-state reaction rapidly eliminated the chemisorbed CO and led to hydrogenation of the stored carbon. Ethane and propane were formed in addition to methane. The rates of formation of these products initially were faster than those observed during steady-state reaction, and the production of hydrocarbons continued long after all of the chemisorbed CO had disappeared from the catalyst surface. Based on these observations it was concluded that molecularly adsorbed CO is not involved in the chain growth process.

The role of surface carbon produced over iron catalysts has been investigated by Bennett et al. (67,68). From their studies the authors concluded that CO is adsorbed dissociatively and that the freshly formed surface carbon is the most abundant surface intermediate. It was noted that the surface carbon serves both as a precursor to the formation of  $\text{Fe}_2\text{C}$  [in addition to other forms of iron carbide (69)] as well as methane and that the latter process is rate-limited by hydrogenation of the carbon intermediate. Additional experiments showed that when a  $\text{C}_2\text{H}_4/\text{H}_2$  mixture was passed over the catalyst following carburization in a  $\text{CO}/\text{H}_2$  mixture the rate of  $\text{CH}_4$ ,  $\text{C}_3\text{H}_8$ , and  $\text{C}_4\text{H}_{10}$  formation was much higher than that observed during the exposure of the catalyst to the  $\text{CO}/\text{H}_2$  mixture. From these results it was inferred that  $\text{CH}_x$  fragments produced from  $\text{C}_2\text{H}_4$  can actively participate in the synthesis of  $\text{C}_{3+}$  alkanes.

The structure and reactivity of carbon deposited on iron surfaces during CO hydrogenation has been investigated further by Bonzel et al. (70-73). Examination of the catalyst surface by Auger and x-ray photoelectron spectroscopies following reaction revealed three types of carbon: a  $\text{CH}_x$  phase; carbidic carbon; and graphitic carbon. The first two types of carbon reacted readily with hydrogen to form methane and  $\text{C}_{2+}$  hydrocarbons, but the graphitic form of carbon was totally unreactive. It was also noted that the rate of hydrogenation of  $\text{CH}_x$  and carbidic carbon corresponded very closely with the initial rate of methane formation from CO and  $\text{H}_2$ . However, the appearance of graphitic carbon led to a suppression of methane synthesis.

Further evidence for the participation of carbidic carbon in the growth of hydrocarbon chains was obtained by Biloen et al. (55). In these studies nickel, cobalt, and ruthenium catalysts were precovered

with  $^{13}\text{C}$  atoms produced by the disproportionation of  $^{13}\text{CO}$ . The remaining adsorbed  $^{13}\text{CO}$  and the catalysts were then exposed to a mixture of  $^{12}\text{CO}$  and  $\text{H}_2$ . As illustrated by the results for nickel shown in Table I, abundant production of  $^{13}\text{CH}_4$  and hydrocarbons containing several  $^{13}\text{C}$  atoms were observed. It was also found that the time needed to convert  $^{13}\text{C}$  atoms and adsorbed  $^{12}\text{CO}$  molecules to methane were nearly identical. From these observations it was concluded that CO dissociation is very rapid and hence kinetically insignificant, that  $\text{CH}_x$  ( $x = 0-3$ ) species constitute the most reactive  $\text{C}_1$  surface species, and that hydrocarbons and methane are formed from the same building blocks, i.e.,  $\text{CH}_x$ .

The fact that surface carbon, produced via CO disproportionation or steady-state hydrogenation, will readily react with hydrogen to produce  $\text{C}_{2+}$  hydrocarbons strongly suggests that carbon-carbon bonds are formed through the reactions of either surface carbon atoms or  $\text{CH}_x$  species. The first of these possibilities seems unlikely since it has been observed that surface carbon once deposited will gradually transform into a less reactive form (e.g., graphitic) if allowed to age in an inert environment (51,52,54). This leads to the proposition that hydrocarbon chain growth proceeds through the polymerization of partially hydrogenated carbon species.

The insertion of methylene segments into the metal-carbon bond of adsorbed alkyl species provides a simple but yet plausible mechanism for chain growth and has been proposed by Biloen et al. (15,55). Precedent for such a reaction pathway has been provided by studies conducted with transition metal complexes. Yamamoto (74) observed that  $\text{CH}_2$  groups could be inserted into the metal-carbon bonds of methyl and ethylnickel complexes by reacting these complexes with  $\text{CH}_2\text{Cl}_2$ . It was also noted

that the reaction of methylnickel complexes with  $\text{CD}_2\text{Cl}_2$  yielded  $\text{CH}_2\text{CD}_2$ , in parallel with earlier work (75) performed with methyliron complexes. The formation of this product was explained by proposing that a  $\text{CD}_2$  group inserts into the  $\text{M}-\text{CH}_3$  bond and that the metal then abstracts a  $\beta$ -hydrogen atom from the resulting alkyl species. The insertion of methylene groups into metal-carbon bonds has also been observed in the work of Young and Whitesides (76) with platinocycloalkanes.

Further evidence for the role of methylene groups in the chain growth process has recently been presented by Brady and Petit (77). It was noted that passage of a dilute stream of  $\text{CH}_2\text{N}_2$  over nickel, palladium, iron, cobalt, ruthenium, and copper catalysts produced predominantly ethylene and nitrogen. When hydrogen was mixed with the  $\text{CH}_2\text{N}_2$  mixture, the nature of the products changed markedly. Over nickel, palladium, cobalt, iron, and ruthenium a mixture of hydrocarbons was produced as shown in Fig. 3. Detailed analyses of the products showed that they consisted mainly of normal alkanes and monoolefins with a distribution closely resembling that found during Fischer-Tropsch synthesis over the same metals. It was further noted that an increase in the hydrogen partial pressure produced a decrease in the chain length and olefin content of the products. Over the copper, the presence of hydrogen did not alter the product spectrum and, hence, mainly ethylene was formed.

Brady and Petit (77) interpret their results in the following fashion. They propose that in the absence of hydrogen the  $\text{CH}_2$  groups released by the decomposition of  $\text{CH}_2\text{N}_2$  dimerize to form ethylene. When hydrogen is present on the catalyst surface, then the  $\text{CH}_2$  groups can undergo hydrogenation to produce methane. The  $\text{CH}_3$  groups formed as a



precursor to methane are assumed to act as chain growth centers. Insertion of a  $\text{CH}_2$  group into the metal-carbon bond of a  $\text{CH}_3$  group produces an ethyl group, and continuation of this type of reaction can give rise to a spectrum of adsorbed alkyl groups. Alkanes are produced by reaction of the alkyl groups with adsorbed hydrogen and olefins are produced by elimination of a  $\beta$ -hydrogen atom from the alkyl groups. In the absence of sufficient atomic hydrogen on the catalyst surface, as might occur on copper, the  $\text{CH}_2$  groups recombine to form ethylene rather than adding hydrogen to form the  $\text{CH}_3$  groups needed to initiate chain growth. On the other hand, if too much atomic hydrogen is available, the extent of chain growth is suppressed.

It is of some interest to contrast the results obtained by Brady and Petit (77) with those obtained earlier by Blyholder and Emmett (78,79). In their studies Blyholder and Emmett introduced a small amount of  $^{14}\text{C}$ -labelled ketene to a  $\text{CO}$  and  $\text{H}_2$  mixture fed over either an iron or cobalt catalyst. When the ketene was labelled in the methylene position a large proportion of the ketene was incorporated into the hydrocarbon products and the radioactivity per mole of product was approximately constant. On the other hand, when the ketene was labelled at the carbonyl position a much smaller fraction of the radioactivity was incorporated into the products but the radioactivity of the products was directly proportional to the number of carbon atoms in the molecule. From these observations, Blyholder and Emmett concluded that ketene undergoes dissociation on the catalyst with the formation of a methylene radical, which initiates chain growth, and carbon monoxide, which contributes to chain growth. This interpretation can be made consistent with the mechanism of hydrocarbon formation proposed by Brady and Petit (77) if one assumes, as shown in

Fig. 4, that ketene decomposes to form predominately methyl rather than methylene groups.

#### PARTICIPATION OF PRIMARY PRODUCTS IN SECONDARY REACTIONS

The discussion presented thus far has focused on those elementary reactions believed to be responsible for the initiation, propagation, and termination of hydrocarbon chain growth. It should be noted that the olefins formed via these primary processes may undergo secondary reactions which can significantly alter the distribution of hydrocarbon chain lengths. Two processes are of interest here, the first being the initiation of new chains and the second being the incorporation of olefins into growing chains.

The early work of Kummer and Emmett (80) and Hall et al. (81) suggested that ethylene can act as a chain initiator on the surface of an iron catalyst. This conclusion was based on the observation that the addition of  $^{14}\text{C}$ -labelled ethylene to the synthesis gas feed led to a constant molar radioactivity of the  $\text{C}_3\text{-C}_5$  fractions. The same result was obtained by Eidus et al. (82) over a cobalt catalyst. Their work showed that 25% of the ethylene was converted to higher hydrocarbons with constant molar radioactivity and that the extent to which ethylene participated as a chain initiator increased in proportion to the amount of ethylene in the gas phase. More recently, Schulz et al. (83) have examined the secondary reactions of  $^{14}\text{C}$ -labelled ethylene, propylene, 1-butene, and 1-hexadecene over both iron and cobalt catalysts. They found that about 90% of the olefin fed reacted. A major portion of the olefin was hydrogenated to the alkane, but  $\alpha$ -olefins were also incorporated into growing chains, initiated new chains, or were cracked to methane. Similar conclusions were drawn by Dwyer and Somorjai (84) based on studies

performed with an Fe (111) surface. Their studies showed that the addition of ethylene or propylene significantly increased the formation of higher molecular weight products. In the case of ethylene the total amount of  $C_3$ - $C_5$  products formed was found to be approximately equal to the conversion of ethylene to hydrocarbons, leading to the conclusion that ethylene incorporates into the growing hydrocarbon chain. The incorporation of olefins during hydrocarbon synthesis over metals other than iron and cobalt has not been investigated in detail but some evidence for this reaction has been observed over ruthenium (85).

The olefins present in the synthesis products may also undergo isomerization and hydrogenation. At high space velocities and low reaction temperatures  $\alpha$ -olefins have been observed as the principal products over iron and ruthenium catalysts (85,86). With increasing temperature and decreasing space velocity, the  $\alpha$ -olefins undergo hydrogenation to form alkanes and isomerization to form  $\beta$ -olefins. The proportion of branched olefins and alkanes formed also depends on the space velocity, leading to the conclusion that these products result from secondary reactions.

#### DETECTION OF REACTION INTERMEDIATES

A number of attempts have been made to identify the intermediates involved in hydrocarbon synthesis by means of in situ infrared spectroscopy. In a study carried out with a silica-supported iron catalyst Blyholder and Neff (87) reported that CH and OH bands observed when the catalyst was heated in a stagnant mixture of CO and  $H_2$  could be ascribed to  $M=C(OH)R$  and  $M-CH_2R$  species. The evidence for the enolic species is not very strong and has recently been questioned by King (88). Working with a silica-supported iron catalyst, the only spectral features he observed were those for structures containing  $CH_2$  and  $CH_3$  groups.

Studies conducted with silica and alumina-supported ruthenium catalysts have also failed to provide clear evidence for reaction intermediates. Dalla Betta and Shelef (89) were able to detect hydrocarbon and formate species on the surface of an alumina-supported catalyst. However, isotopic substitution experiments, in which  $H_2$  was replaced by  $D_2$  in the reactant feed stream, led to the conclusion that the observed structures were inactive reaction products apparently adsorbed on the alumina support. Similar conclusions were drawn by Ekerdt and Bell (66) from studies conducted with a silica-supported ruthenium catalyst. In this instance, only hydrocarbon species were observed. While these structures did not undergo elimination or deuterium substitution under reaction conditions, they could be removed from the catalyst by reduction with  $H_2$  in the absence of CO. Based on these observations it was concluded that the observed species are attached to the surface of ruthenium but are inactive in the formation of light hydrocarbon products. Studies conducted by King (88) have also confirmed this conclusion. However, King has suggested that the hydrocarbon species observed by infrared spectroscopy may be associated with the formation of high molecular weight liquids or waxes rather than light gases. Tamaru (90), on the other hand, has recently shown that the accumulated hydrocarbon species can undergo hydrogenolysis and, as a result, has suggested that the observed species may act as a reservoir for  $CH_x$  groups.

Inelastic electron tunneling spectroscopy has been used by Kroeker et al. (91) to look for hydrocarbon intermediates on the surface of an alumina-supported rhodium catalyst. The vibrational spectra obtained by this means showed strong evidence for an ethylidene species and a second structure believed to be a formate ion. Studies with  $^{13}C^{16}O$  and  $^{12}C^{18}O$  confirmed that the ethylidene structure was formed via CO hydrogenation but the role of this structure as an intermediate was not established.

A chemical technique for detecting surface intermediates has recently been investigated by Bell et al. (92,93). The principal of the approach, referred to as reactive scavenging of surface intermediates, is illustrated in Fig. 5 and is based on reports that both alkylidene (94-96) and alkyl ligands (97) can be eliminated from metal complexes by reaction with olefins. In practice a small amount (< 2%) of ethylene or cyclohexene is added to the synthesis gas feed. The reaction products are then collected and analyzed by gas chromatography/mass spectrometry. Ekerdt and Bell (92) observed that the addition of ethylene to the feed during synthesis over a silica-supported ruthenium catalyst enhanced the formation of propylene. When cyclohexene was added to the feed, methyl- and ethylcyclohexene and ethyl-, propyl-, and butylcyclohexane were detected. Significantly, the addition of cyclohexene produced only small changes in the distribution of products obtained from CO hydrogenation. Subsequent studies with cyclohexene addition conducted by Baker and Bell (93) have shown that norcarane can be formed in addition to the alkyl derivatives of cyclohexane and cyclohexene and that the concentrations of these products are sensitive to the conditions under which synthesis is carried out, as is illustrated in Table II.

The appearance of propylene when ethylene is used as the scavenging agent and norcarane when cyclohexene is used provide very strong evidence for the presence of methylene groups on the surface of the ruthenium catalyst. The detection of alkyl cyclohexenes and alkyl cyclohexanes can be explained by the reaction of cyclohexene with either alkyl or alkylidene species (92). Moreover, the fact that the yield of scavenged products depends on the synthesis conditions supports the contention that the olefin additives react with intermediates involved in the synthesis of hydrocarbons. Further evidence supporting this conclusion has been

reported recently by Tamaru (90). In these studies a small amount of ethylene was added to a mixture of  $^{13}\text{C}\text{O}$  and  $\text{H}_2$  passed over a silica-supported ruthenium catalyst. Scavenging of  $\text{CH}_2$  groups from the catalyst surface was evidenced by the detection of  $^{13}\text{C}^{12}\text{C}_2\text{H}_6$ . The absence of any propylene containing two or three  $^{12}\text{C}$  atoms indicates that the ethylene did not act as a source of  $\text{CH}_2$  groups.

#### PROPOSALS FOR A REACTION MECHANISM AND DISCUSSION OF ITS IMPLICATIONS

The discussion presented in the preceding sections suggest that the synthesis of hydrocarbons from  $\text{CO}$  and  $\text{H}_2$  can be described by the reaction network shown in Fig. 10. In the first steps of this mechanism  $\text{CO}$  chemisorbs molecularly and then dissociates to produce atoms of carbon and oxygen. The extent to which these processes are reversible is not yet fully understood. However, temperature programmed desorption experiments conducted with ruthenium (98) indicate that the recombination of carbon and oxygen atoms and the desorption of  $\text{CO}$  are very rapid since extensive scrambling of preadsorbed  $^{13}\text{C}^{16}\text{O}$  and  $^{12}\text{C}^{18}\text{O}$  is observed at temperatures where hydrocarbon synthesis normally occurs. Hydrogen chemisorption is also taken to be reversible, based on experiments which show that desorption is rapid at reaction temperatures (99).

The oxygen released by  $\text{CO}$  dissociation is removed from the catalyst as either  $\text{H}_2\text{O}$  or  $\text{CO}_2$ . Which of these two products predominates depends very much upon catalyst composition. Thus,  $\text{H}_2\text{O}$  is the dominant product observed using cobalt and ruthenium catalysts, a mixture of  $\text{H}_2\text{O}$  and  $\text{CO}_2$  is obtained using an unpromoted iron catalyst, and  $\text{CO}_2$  is the dominant product found when iron and cobalt catalysts are promoted with potassium (3). Details of the mechanistic steps involved in oxygen removal under hydrocarbon synthesis conditions are not well established and hence both Eley-Rideal and Langmuir-Hinshelwood type processes should be considered.

As discussed previously it seems reasonable to suggest that the synthesis of hydrocarbons is initiated by the stepwise hydrogenation of single carbon atoms. The methyne, methylene, and methyl groups produced by this means are assumed to be in equilibrium based on the results of studies with iron and osmium clusters containing these species as ligands (58,59,61). Hydrogen-deuterium substitution studies conducted with ruthenium catalysts (100) also support this assumption and are discussed in detail below. The methyl groups are viewed as precursors to both methane formation and chain growth. The former process occurs with the addition of a hydrogen atom and the latter with the insertion of a methylene group into the M-C bond of the methyl group. Once started, chain growth can continue by further addition of methylene units to the alkyl intermediates. Termination of chain growth is postulated to occur via one of two processes - hydrogen addition to form normal alkanes and  $\beta$ -elimination of hydrogen to form  $\alpha$ -olefins. Thus, one may visualize the formation of  $C_{2+}$  hydrocarbons as a polymerization process in which the methylene groups act as the monomer and the alkyl groups are the active centers for chain growth.

The mechanism illustrated in Fig. 6 describes only the primary process leading to hydrocarbons and neglects the formation of oxygenated products. If the concentration of hydrocarbons in the gas phase is sufficiently high, then a number of secondary processes can occur. Most significant would be the addition of olefins to form longer chain products and the hydrogenation of olefins to form alkanes. The formation of oxygenated species could be envisioned to occur via reactions such as those shown in Fig. 7. In this instance direct hydrogenation of a CO molecule bonded through both its carbon and oxygen ends could lead to the formation of methoxide species which might serve as a precursor to

methanol. The insertion of a CO molecule into a metal-alkyl bond and subsequent addition of hydrogen could provide pathways for the formation of aldehydes and higher alcohols. While the chemistry shown in Fig. 11 is plausible and consistent, at least in part with reactions known to occur with transition metal complexes (56,101), its substantiation with respect to Fischer-Tropsch synthesis has not been explored in much detail.

In a series of recent studies, Kellner and Bell (102) have examined the implication of the mechanism outlined in Fig. 10 for the kinetics of hydrocarbon synthesis over ruthenium. To obtain tractable rate expressions, a number of simplifying assumptions were introduced. The first is that under reaction conditions the catalyst surface is nearly saturated by chemisorbed CO. This assumption is supported by in situ infrared observations carried out at both low and high pressure (66,88,89). The second assumption is that water is the primary product through which oxygen is removed from the catalyst surface and that the formation of water takes place via an Eley-Rideal mechanism. While experimental evidence (3,66,102) confirms the formation of water as the primary oxygen containing species, the mechanism of its formation has not been established. The third assumption is that all of the steps shown to be reversible are, in fact, at equilibrium. The fourth, and final, assumption is that the probability of chain propagation is independent of chain length.

Two limiting forms can be derived for the kinetics of methane synthesis, depending on whether methane or higher molecular weight hydrocarbons predominate among the products formed. In the first case, the rate of methane formation is given by

$$N_{C_1} = k_e P_{H_2}^{1.5} / P_{CO} \quad (1)$$

where



$$k_e = \frac{K_3}{K_1} (k_4 k_8 K_5 K_6 K_7)^{1/2} \quad (2)$$

and in the second case by

$$N_{C_1} = k_e P_{H_2}^{1.5} / P_{CO}^{1.33}, \quad (3)$$

where

$$k_e = k_8 \left[ \frac{k_4 K_2 K_3^{3.5} K_5 K_6 K_7^2 (1-\alpha)}{k_p k_1^4} \right]^{1/3} \quad (4)$$

The dependence of  $N_{C_1}$  on the partial pressures of  $H_2$  and  $CO$  exhibited in eqns. 1 and 3 can now be compared with those observed experimentally.

Correlation of methane formation rates obtained at pressures between 1 and 10 atm, temperatures between 175 and 275°C, and  $H_2/CO$  ratios between 1 and 3 leads to an expression of the form (101)

$$N_{C_1} = k_e P_{H_2}^{1.35} / P_{CO}^{0.99}, \quad (5)$$

where

$$k_e = 7.5 \times 10^8 \exp(28,000/RT), \text{ s}^{-1}. \quad (6)$$

While the content of methane in the products over the indicated range of conditions varies from 20 to 40 weight percent, the form of eqn. 5 is most nearly like that given by eqn. 1.

Working with the same catalysts used to study the kinetics of methane synthesis, Kellner and Bell (100) investigated the effects of substituting  $D_2$  for  $H_2$  in the synthesis mixture. A strong inverse isotope effect of magnitude 1.4 to 1.5 was observed both at 1 and 10 atm for an alumina-supported ruthenium catalyst. When silica was used as the support, the effect was 1.1 at 10 atm and became negligible at 1 atm.

The origin of the isotope effect and its magnitude can be explained on the basis of the mechanism of methane formation proposed in Fig. 6. The fact that some of the elementary processes are at equilibrium while others are not means that the overall isotope effect will consist of a combination of equilibrium and kinetic isotope effects. This conclusion is further indicated by the structure of the effective rate coefficient,  $k_e$ , given by either eqn. 2 or 4. As discussed by Kellner and Bell (100), the equilibrium constants for the stepwise hydrogenation of surface carbon to  $\text{CH}_3$  species are favored when  $\text{D}_2$  rather than  $\text{H}_2$  is used, but the equilibrium constant for  $\text{D}_2$  adsorption is smaller than that for  $\text{H}_2$  adsorption at reaction temperature. By contrast, rate coefficients for processes involving the addition of hydrogen are expected to be larger in the presence of  $\text{H}_2$  than  $\text{D}_2$ . In view of these considerations and the form of eqns. 2 and 4, it is seen that the equilibrium and kinetics isotope effects counteract each other. The existence of a strong inverse isotope effect over alumina-supported ruthenium indicates that the equilibrium component of the overall effect is dominant. However, for the silica-supported catalyst the balance between equilibrium and kinetic isotope effects is more nearly equal and hence the overall effect is smaller.

Rate expressions for the synthesis of hydrocarbons containing two or more carbon atoms can also be derived from the proposed mechanism (102). If it is assumed that the probability of chain propagation,  $\alpha$ , is independent of chain length,  $n$ , then the rate of formation of hydrocarbons containing  $n$  atoms can be expressed as

$$N_{C_n} = N_{C_n}^+ + N_{C_n}^- \quad (7)$$

$$= (k_{to v} + k_{tp H}) \alpha^{n-1} \theta_{CH_3} \quad (8)$$

$$= \left(1 + \frac{k_{to v}}{k_{tp H}}\right) \alpha^{n-1} k_{tp H} \theta_{CH_3} \quad (9)$$

where  $k_{to}$  and  $k_{tp}$  are the rate coefficients for termination of chain growth by formation of olefins and paraffins,  $\theta_v$  is the fraction of the catalyst surface which is vacant, and  $\theta_H$  and  $\theta_{CH_3}$  are the fractions of the surface covered by H atoms and  $CH_3$  groups. The second term in the parentheses of eqn. 9 can be written as

$$\begin{aligned} \frac{k_{to v}}{k_{tp H}} &= \frac{k_{to}}{k_{tp} K_3^{1/2} P_{H_2}^{1/2}} \quad (10) \\ &= \beta / P_{H_2}^{1/2} \end{aligned}$$

Substitution of eqn. 10 and the expression given in eqn. 11 for the rate of methane formation into eqn. 9

$$N_{C_1} = k_8 \theta_H \theta_{CH_3} \quad (11)$$

leads to a statement for the rate of synthesis of hydrocarbons containing  $n$  atoms.

$$N_{C_n} = \frac{k_{tp}}{k_8} \left(1 + \beta / P_{H_2}^{1/2}\right) \alpha^{n-1} N_{C_1} \quad (12)$$

From a comparison of eqn. 7 and eqn. 12 it may be concluded further that the ratio olefins to paraffins can be expressed as

$$\frac{N_{C_n}}{N_{C_1}} = \beta / P_{H_2}^{1/2} \quad (13)$$

The dependence of the propagation probability,  $\alpha$ , on the partial pressures of  $H_2$  and CO can also be deduced. The defining expression for  $\alpha$  is

$$\alpha = \frac{k_p \theta_{CH_2}}{(k_p \theta_{CH_2} + k_{to} \theta_v + k_{tp} \theta_H)} \quad (14)$$

By introduction of the appropriate expressions for  $\theta_{CH_2}$ ,  $\theta_H$ , and  $\theta_v$ , it can be demonstrated (101) that eqn. 14 can be rewritten as

$$\alpha = [1 + \gamma P_{CO}^{-0.67} (1 + \beta P_{H_2}^{-0.5})]^{-1} \quad (15)$$

where  $\gamma$  is given by

$$\gamma = \left[ \frac{K_3}{k_p^2 k_4 (1-\alpha) K_1^2 K_2 K_5 K_6} \right]^{1/3} \quad (16)$$

The form of eqn. 12 indicates that a plot of  $\log(N_{C_n}/N_{C_1})$  versus  $(n-1)$  should be linear with a slope of  $\log \alpha$ . Figure 8 illustrates three such plots for data taken at 1 atm and 275°C (102). It is apparent that with the exception of the point for  $C_2$  hydrocarbons, the data fall along a straight line. The values of  $\alpha$  determined from the slopes are 0.47, 0.51, and 0.56 for  $H_2/CO$  ratios of 3, 2, and 1 correspondingly. The observed increase in  $\alpha$  with increasing  $H_2/CO$  ratio at a fixed total pressure is properly predicted by eqn. 16. Data taken at other temperatures and pressures also fall along a straight line when plotted as  $\log(N_{C_n}/N_{C_1})$  versus  $(n-1)$ : the primary difference being that the values of  $\alpha$  for data

taken at higher pressures (e.g., 10 atm) are less sensitive to changes in temperature and  $H_2/CO$  ratio than for data taken at 1 atm.

A test of the expression for the olefin to paraffin ratio eqn. 13,, is shown in Fig. 9. The data plotted in this figure were taken at 225°C, pressures between 1 and 10 atm, and  $H_2/CO$  ratios of 3 to 1. As may be seen, the olefin to paraffin ratios for  $C_2$  through  $C_4$  hydrocarbons are proportional to  $P_{H_2}^{-0.5}$ , as predicted by eqn. 13. A similar relationship was also observed for  $C_5$  through  $C_{10}$  hydrocarbons. It is to be noted, however, that in contrast with the assumptions underlying the derivation of eqn. 13,  $\beta$  is found to be a function of  $n$ . This is seen both in Fig. 14 and even more clearly in Table III. The implication of this observation is that the ratio of the termination rate coefficients depends on the number of carbon atoms in the alkyl group.

#### CONCLUDING REMARKS

In the field of catalysis it is well recognized that it is extremely difficult to demonstrate the predominance of a single reaction mechanism to the exclusion of all other alternatives, and as a result, mechanistic discussions rarely lead to a definitive identification of a particular reaction pathway. From this perspective, we must conclude that the discussion presented here does not constitute a proof of the mechanism of hydrocarbon synthesis proposed in Fig. 10 but, rather, only strong support for its validity. The intermediates invoked have been shown to exist as ligands in transition metal complexes and, in at least one case, have been identified during reaction by the technique of reactive scavenging. Likewise, precedents have been shown to exist for essentially all of the elementary processes. Of additional significance

is the fact that the proposed mechanism leads in a rational fashion to a series of expressions which properly characterize the kinetics of hydrocarbon synthesis over ruthenium.

It is anticipated that future studies will help to achieve an even more detailed picture of the reaction mechanism. Such efforts should help to establish how the nature of the most abundant surface species changes with changes in catalyst composition and how catalyst composition and/or reaction conditions affect the identity of rate-limiting steps. It will also be important to determine more clearly the role which secondary reactions, involving olefins, play in shaping the overall product distribution. Finally, development of a better understanding of the processes leading to oxygenated products should be undertaken in order to elucidate what factors control the formation of these products instead of hydrocarbons.

#### ACKNOWLEDGMENT

This work was supported by the Division of Chemical Sciences, Office of Basic Energy Sciences, U.S. Department of Energy under Contract W-7405-Eng-48.

## REFERENCES

1. F. Fischer and H. Tropsch, Chem. Ber., 59, 830 (1926).
2. F. Fischer and H. Tropsch, Brennst. Chem. 7, 97 (1926).
3. H. H. Storch, N. Golumbic, and R. B. Anderson, The Fischer-Tropsch and Related Syntheses, Wiley, New York, 1951.
4. H. Pichler, Adv. Catal., 4, 271 (1952).
5. R. B. Anderson, in Catalysis, Vol. 4 (P. H. Emmett, ed.) Rheinhold, New York, 1956.
6. B. K. Nefedov and Ya. T. Eidus, Russ. Chem. Rev., 34, 272 (1965).
7. Ya. T. Eidus, Russ. Chem. Rev., 36, 338 (1967).
8. V. M. Vlasenko and G. E. Yuzefovich, Russ. Chem. Rev., 38, 728 (1969).
9. H. Pichler and H. Schulz, Chem. Ing. Tech., 42, 1162 (1970).
10. H. Pichler, Erdoel Kohle, Erdgas, Petrochem. Brennst. Chem., 26, 625 (1973).
11. G. A. Mills and F. W. Steffgen, Catal. Rev. Sci. Eng., 8, 159 (1973).
12. M. A. Vannice, Catal. Rev. Sci. Eng., 14, 153 (1976).
13. V. Ponec, Catal. Rev. Sci. Eng., 18, 151 (1978).
14. V. Ponec and W. A. von Barneveld, I&EC Prod. Res. Develop., 18, 268 (1979).
15. P. Biloen, J. Roy. Neth. Chem. Soc., 99, 33 (1980).
16. S. R. Craxford and E. K. Rideal, J. Chem. Soc., 1, 604 (1939).
17. S. R. Craxford, Fuel, 26, 119 (1946).
18. S. R. Craxford, Trans. Farad. Soc., 42, 576 (1946).
19. J. T. Kummer, T. W. DeWitt, and P. H. Emmett, J. Amer. Chem. Soc., 70, 2632 (1948).
20. J. T. Kummer, L. C. Browning, and P. H. Emmett, J. Chem. Phys., 16, 739 (1948).
21. L. C. Browning, T. W. DeWitt, and P. H. Emmett, J. Am. Chem. Soc., 72, 4211 (1950).

22. Ya. T. Eidus, Izv. Akad. Nauk SSSR, Otd. Khim. Nauk., 129 (1951).
23. H. Pichler and H. Buffleb, Brennst. Chem., 21, 257, 273, 285 (1940).
24. A. W. Sternberg and I. Wender, Proc. Intern. Conf. Coordin. Chem., 53, The Chem. Soc., London (1959).
25. C. L. Allyn, T. Gustaffson, E. W. Plummer, Chem. Phys. Lett., 47, 127 (1977).
26. G. Broden, T. N. Rhodin, and C. Brucker, Surface Sci., 59, 593 (1976).
27. I. P. Batra and O. Robaux, J. Vac. Sci. Technol., 12, 242 (1975).
28. L. H. Little, Infrared Spectra of Adsorbed Species, Academic Press, New York (1966).
29. G. Blyholder, J. Phys. Chem., 74, 4335 (1970).
30. K. C. Lin, J. D. Witt, R. M. Hammaker, J. Chem. Phys., 55, 1148 (1971).
31. A. Cossley and D. A. King, Surface Sci., 68, 528 (1977).
32. G. Blyholder, J. Phys. Chem., 68, 2772 (1964).
33. G. Blyholder, J. Phys. Chem., 79, 756 (1975).
34. G. Doyen and G. Ertl, Surface Sci., 43, 197 (1974).
35. I. P. Batra and P. S. Bagus, Solid State Commun., 16, 1097 (1975).
36. L. S. Cederbaum, W. Domcke, W. von Niessen, and W. Brenig, Z. Physik., B21, 381 (1975).
37. G. Blyholder, J. Vac. Sci. Technol., 11, 865 (1974).
38. C. R. Guerra and J. H. Schulman, Surface Sci., 7, 229 (1967).
39. C. R. Guerra, J. Colloid. Interface Sci., 29, 229 (1969).
40. H. Wise, Stanford Research Institute, Menlo Park, CA, personal communication.
41. M. Manassero, M. Sansoni, and G. Longani, J. C. S. Chem. Comm., 1919 (1976).



42. N. V. Richardson and A. M. Bradshaw, Surface Sci., 88, 255 (1979).
43. M. Araki and V. Ponec, J. Catal., 44, 439 (1976).
44. W. L. von Dijk, J. A. Groenewegen, and V. Ponec, J. Catal., 45, 277 (1976).
45. V. Ponec, Catal. Rev., 11, 1 (1975).
46. J. C. Robertson and C. W. Wilmsen, J. Vac. Sci. Technol., 9, 901 (1972).
47. E. Miyazaki, J. Catal., in press.
48. D. W. Goodman and J. M. White, Surface Sci., 90, 201 (1979).
49. D. W. Goodman, R. D. Kelley, T. E. Madey, and J. M. White, J. Vac. Sci. and Technol., 17, 143 (1980).
50. D. W. Goodman, R. D. Kelley, T. E. Madey, and J. T. Yates, Jr., J. Catal.,
51. J. G. McCarty and H. Wise, J. Catal., 57, 406 (1979).
52. P. R. Wentrcck, B. J. Wood, H. Wise, J. Catal., 43, 363 (1976).
53. J. A. Rabo, A. P. Risch, and M. L. Poutsma, J. Catal., 53, 295 (1978).
54. G. Low and A. T. Bell, J. Catal., 57, 397 (1979).
55. P. Biloen, J. N. Helle, and W. M. H. Sachtler, J. Catal., 58, 95 (1979).
56. E. L. Muetterties and J. Stein, Chem. Rev., 80, 479 (1979).
57. J. E. Demuth and H. Ibach, Surface Sci., 78, L238 (1978).
58. J. E. Demuth, Surface Sci., 93, 127 (1980).
59. M. Tachikawa and E. L. Muetterties, J. Am. Chem. Soc., in press.
60. M. A. Beno, J. M. Williams, M. Tachikawa, and E. L. Muetterties, J. Am. Chem. Soc., in press.
61. R. B. Calvert and J. R. Shapley, J. Am. Chem. Soc., 99, 5226 (1977).
62. R. B. Calvert and J. R. Shapley, A. J. Schultz, J. M. Williams, S. L. Suib, and G. D. Stucky, J. Am. Chem. Soc., 100, 6240 (1978).
63. R. B. Calvert and J. R. Shapley, J. Am. Chem. Soc., 100, 7727 (1978).
64. C. E. Sumner, Jr., P. E. Riley, R. E. Davis, and R. Petit, J. Am. Chem. Soc., 102, 1752 (1980).
65. C. R. Eady, B. F. G. Johnson, and J. Lewis, J. Chem. Soc. Dalton Trans., 477 (1977).

66. J. G. Ekerdt and A. T. Bell, J. Catal., 58, 170 (1979).
67. H. Matsumoto and C. O. Bennett, J. Catal., 53, 331 (1978).
68. J. P. Reymond, P. Mérideau, B. Pommier, and C. O. Bennett, J. Catal., 64, 163 (1980).
69. K. M. Sawcier, W. E. Isakson, and H. Wise, Adv. Chem. Series, No. 178, 129 (1979).
70. H. P. Bonzel and H. J. Krebs, Surface Sci., 91, 449 (1980).
71. H. P. Bonzel and H. J. Krebs, Preprints ACS Div. Fuel Chem., 25, 19 (1980).
72. H. J. Krebs and H. P. Bonzel, Surface Sci., in press.
73. H. P. Bonzel, H. J. Krebs, and W. Schwarting, Chem. Phys. Lett., in press.
74. T. Yamamoto, J. Chem. Soc. Chem. Commun., 1003 (1978).
75. T. Ikariya and A. Yamamoto, J. Chem. Soc. Chem. Commun., 720 (1974).
76. C. B. Young and G. M. Whitesides, J. Am. Chem. Soc., 100, 5808 (1978).
77. R. C. Brady, III and R. Pettit, J. Am. Chem. Soc., in press.
78. G. Blyholder and P. H. Emmett, J. Phys. Chem., 63, 962 (1959).
79. G. Blyholder and P. H. Emmett, J. Phys. Chem., 64, 470 (1960).
80. J. T. Kummer and P. H. Emmett, J. Am. Chem. Soc., 75, 5177 (1953).
81. W. K. Hall, R. J. Kokes, and P. H. Emmett, J. Am. Chem. Soc., 82, 1027 (1960).
82. Ya. T. Eidus, N. D. Zelinskii, and N. I. Erskov, Dokl. Akad. Nauk. SSSR., 60, 599 (1948).
83. H. Schulz, B. R. Rao, and M. Elstner, Erdol Kohle, 23, 651 (1970).
84. D. J. Dwyer and G. A. Somorjai, J. Catal., 56, 249 (1979).
85. S. C. Kellner and A. T. Bell, unpublished results.
86. H. Pichler, H. Schulz, and F. Hojabri, Brennst. Chem., 45, 215 (1964).
87. G. Blyholder and L. D. Neff, J. Phys. Chem., 66, 1664 (1962).
88. D. L. King, J. Catal., 61, 77 (1980).
89. R. A. Dalla Betta and M. Shelef, J. Catal., 48, 111 (1977).
90. K. Tamaru, Preprints, The Seventh International Congress on Catalysis, Tokyo, 1980.

91. R. M. Kroeker, W. C. Kaska, and P. K. Hansma, J. Catal., 61, 87 (1980).
92. J. G. Ekerdt and A. T. Bell, J. Catal., 62, 19 (1980).
93. J. Baker and A. T. Bell, unpublished results.
94. J. D. Fellman, G. A. Rupprecht, C. D. Wood, and R. R. Schrock,  
J. Amer. Chem. Soc., 100, 5962 (1978).
95. A. E. Stevens and J. L. Beauchamp, J. Amer. Chem. Soc., 100, 2584 (1978).
96. R. H. Grubbs and A. Miyashita, J. Amer. Chem. Soc., 100, 7418 (1978).
97. E. R. Evitt and R. G. Bergman, J. Amer. Chem. Soc., 101, 3973 (1979).
98. J. G. McCarty and H. Wise, Chem. Phys. Letters, 61, 323 (1979).
99. M. Uchida and A. T. Bell, J. Catal., 60, 204 (1979).
100. S. C. Kellner and A. T. Bell, J. Catal., in press.
101. H. Kung, Catal. Rev. Sci. Eng., in press.
102. S. C. Kellner and A. T. Bell, submitted to J. Catal.

Table 1

Isotopic Composition of Methane and Higher Hydrocarbons<sup>a</sup>(55)

Series	Batch	$\delta^{13}\text{C}$	$\text{CH}_4$		$\text{C}_2\text{H}_6$			$\text{C}_2\text{H}_8^b$				$\text{C}_4\text{H}_{10}$				
			0 <sup>b</sup>	1	0	1	2	0	1	2	3 <sup>b</sup>	0	1	2	3	4
11	1	0.62	44 <sup>d</sup>	56	45	46	9	16	30	37	17 <sup>c</sup>					
	2	0.50	42	58	48	39	13	32	34	27	7					
	4	0.32	76	24	61	29	10	61	26	13	-					
	5	0.24	82	18	75	25	-	63	26	11	-					
5	1	0.36	38	62	49	30	21	31	27	28	14					
	2	0.27	54	46	51	30	19	55	26	14	6					
20	2	0.20	75	25	60	23	17	61	25	14	-	28	28	21	13	-
	3	0.13	86	14	78	22	-	73	21	6	-	48	26	24	-	-

<sup>a</sup> 4 wt% Ni/SiO<sub>2</sub>; T = 170°C; P = 1 bar; H<sub>2</sub>/CO molar ratio = 3.

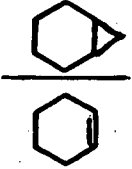
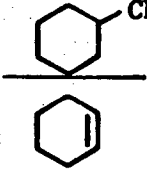
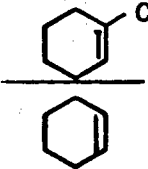
<sup>b</sup> Number of all C<sub>3</sub>H<sub>8</sub> molecules are <sup>13</sup>C<sub>3</sub>H<sub>8</sub> molecules.

<sup>c</sup> 17 mol% of <sup>13</sup>C atoms per molecule.

<sup>d</sup> Data given in mole percent.

Table II

Effect of  $H_2/CO$  Ratio in the Synthesis Gas  
on the Distribution of Scavenger Products<sup>a</sup>(92)

$H_2/CO$			
3	$3.6 \times 10^{-4}$	$2.1 \times 10^{-5}$	$1.9 \times 10^{-5}$
6	$5.9 \times 10^{-4}$	$3.3 \times 10^{-5}$	$4.1 \times 10^{-5}$
9	$4.3 \times 10^{-4}$	$1.1 \times 10^{-4}$	$8.7 \times 10^{-5}$

<sup>a</sup> 4 wt% Ru/SiO<sub>2</sub>; T = 225°C; P = 1 atm.

Table III

Dependence of  $\beta$  on  $n^a$  (101)

<u>n</u>	<u><math>\beta_n</math></u>
2	8.7
3	10.9
4	5.8
5	5.1
6	7.2
7	5.7
8	4.9
9	4.2
10	3.1

---

<sup>a</sup> 1 wt% Ru/Al<sub>2</sub>O<sub>3</sub>; T = 225°C; P = 10 atm.

- Fig. 1 A section of the Periodic Table showing the room temperature adsorption behavior of CO. M denotes molecular adsorption and D dissociative adsorption on one surface, single crystal or polycrystalline. The thick line defines the borderline between molecular and dissociative adsorption at room temperature. The numbers on the third line of each block show the average value for the energy separation of the 4 and 1 UPS peaks,  $\Delta(1\pi-4\sigma)$ . The numbers on the fourth line of each block show the activation energy for dissociative chemisorption of CO from the molecular state determined from Bond Energy Bond Order calculations. The form of CO adsorption at room temperature and values of  $\Delta(1\pi-4\sigma)$  are taken from ref. (26) and the values of the activation energy for dissociation from ref. (47).
- Fig. 2 An energy level diagram for the molecular and dissociative chemisorption of CO on nickel and ruthenium.
- Fig. 3 Reactions of diazomethane on transition metal surfaces. Redrawn from ref. (26).
- Fig. 4 Proposed reaction pathways for the incorporation of fragments derived from  $^{14}\text{C}$  labelled ketene, during Fischer-Tropsch synthesis.
- Fig. 5 A schematic illustration of reactive scavenging of surface intermediates.
- Fig. 6. A proposed mechanism for hydrocarbon synthesis from CO and  $\text{H}_2$  over group VIII metals.
- Fig. 7. Possible reaction sequences leading to the formation of oxygenated products.
- Fig. 8. Plots of  $\log(N_{\text{C}_n}/N_{\text{C}_1})$  versus  $(n-1)$  for different  $\text{H}_2/\text{CO}$  feed ratios.
- Fig. 9. Plots of  $N_{\text{C}_n}^+ / N_{\text{C}_n}^-$  versus  $P_{\text{H}_2}^{-1/2}$  for  $n = 2, 3, \text{ and } 4$ .

III B	IV B	V B	VI B	VII B	VIII	VIII	VIII	IB
Sc	Ti	V	Cr	Mn	Fe	Co	Ni	Cu
-	D	-	-	-	D	-	M	-
-	-	-	-	-	3.5	-	3.08	-
-	2.5	1.7	4.2	3.3	15.9	23.4	23.4	-
Y	Zr	Nb	Mo	Tc	Ru	Rh	Pd	Ag
-	-	-	D	-	M	-	M	-
-	-	-	3.5	-	3.15	-	2.90	-
-	0	0	5.8	20.9	43.4	49.3	58.5	-
La	Hf	Ta	W	Re	Os	Ir	Pt	Au
-	-	-	D,M	-	-	M	M	-
-	-	-	3.2	-	-	2.75	2.60	-
-	0	0	0	15.9	36.7	41.8	49.3	-

Figure 1



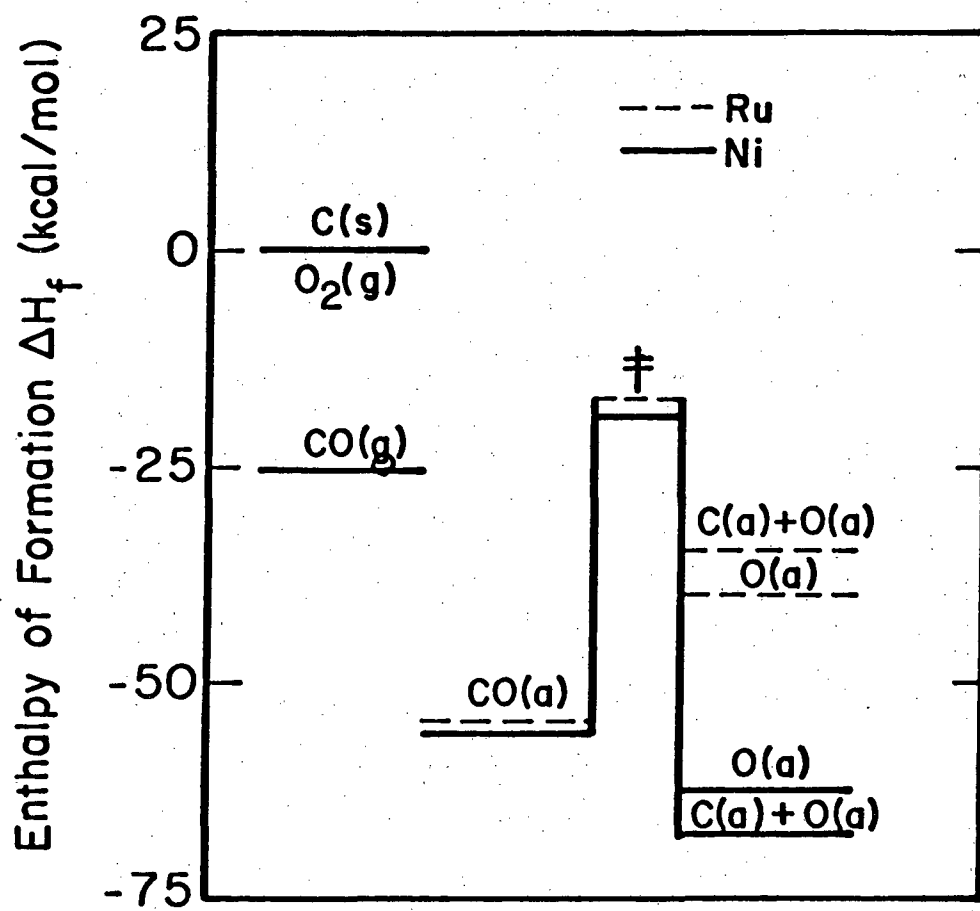


Figure 2

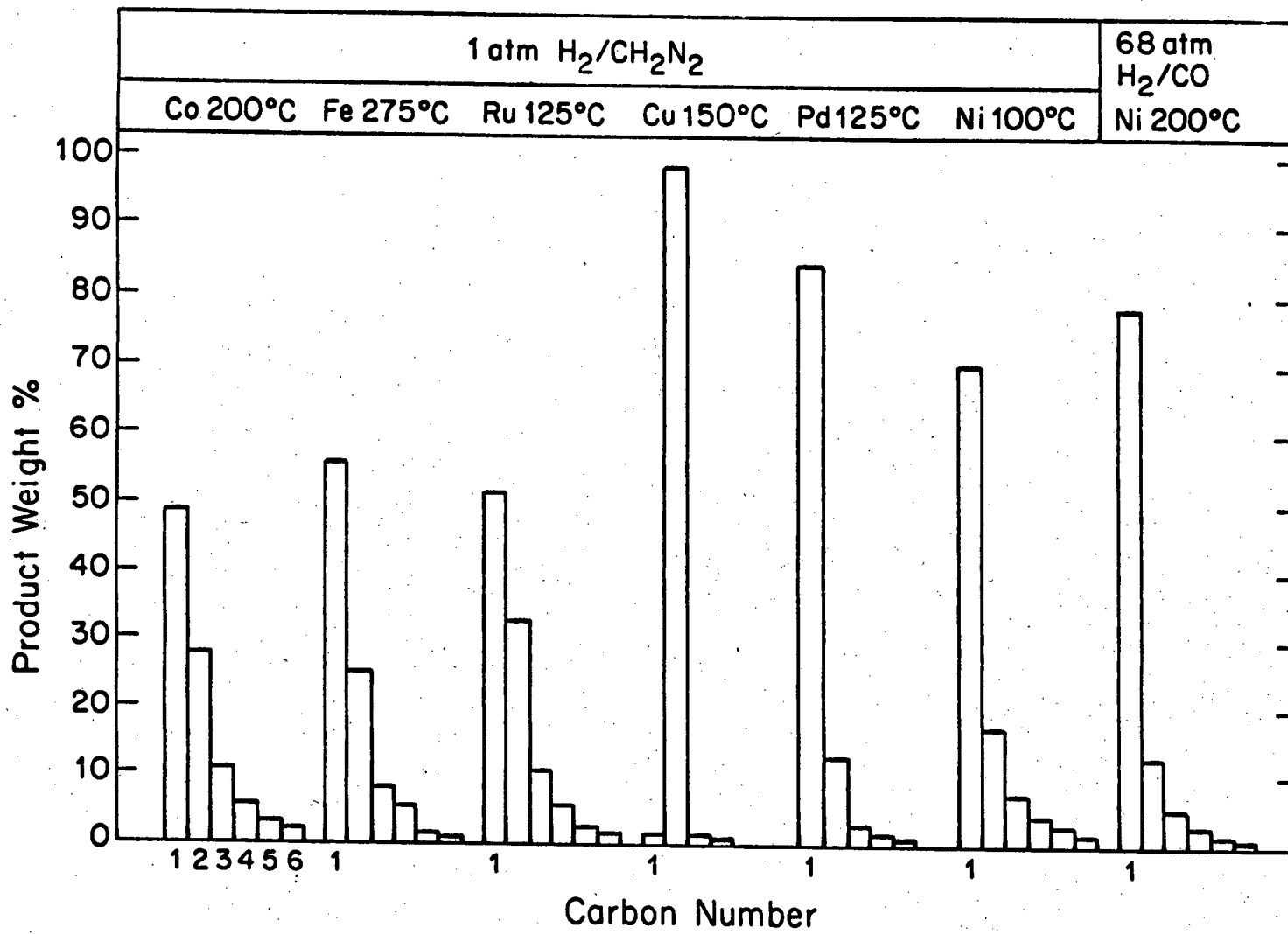


Figure 3

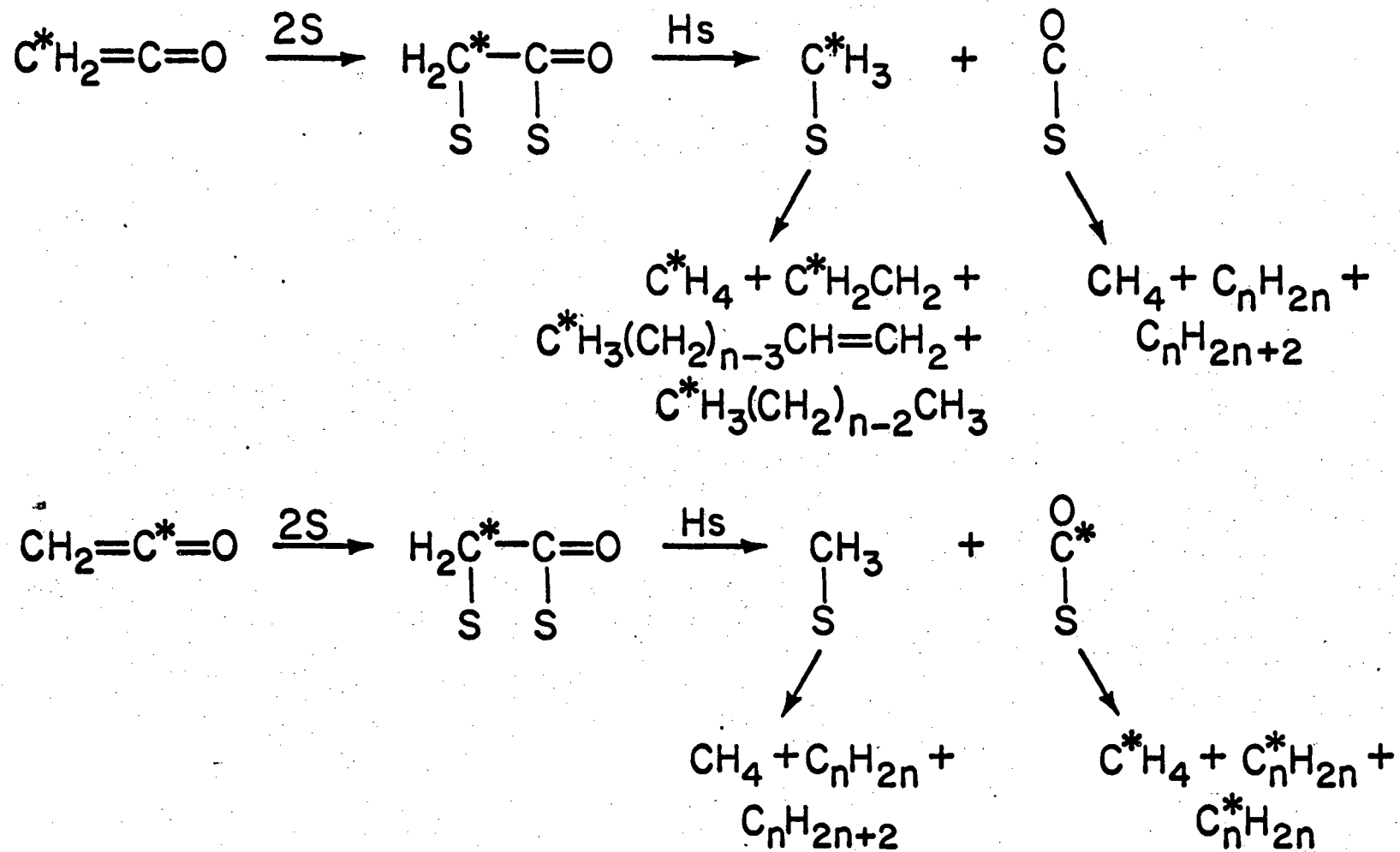


Figure 4

## Reactive Scavenging of Surface Intermediates

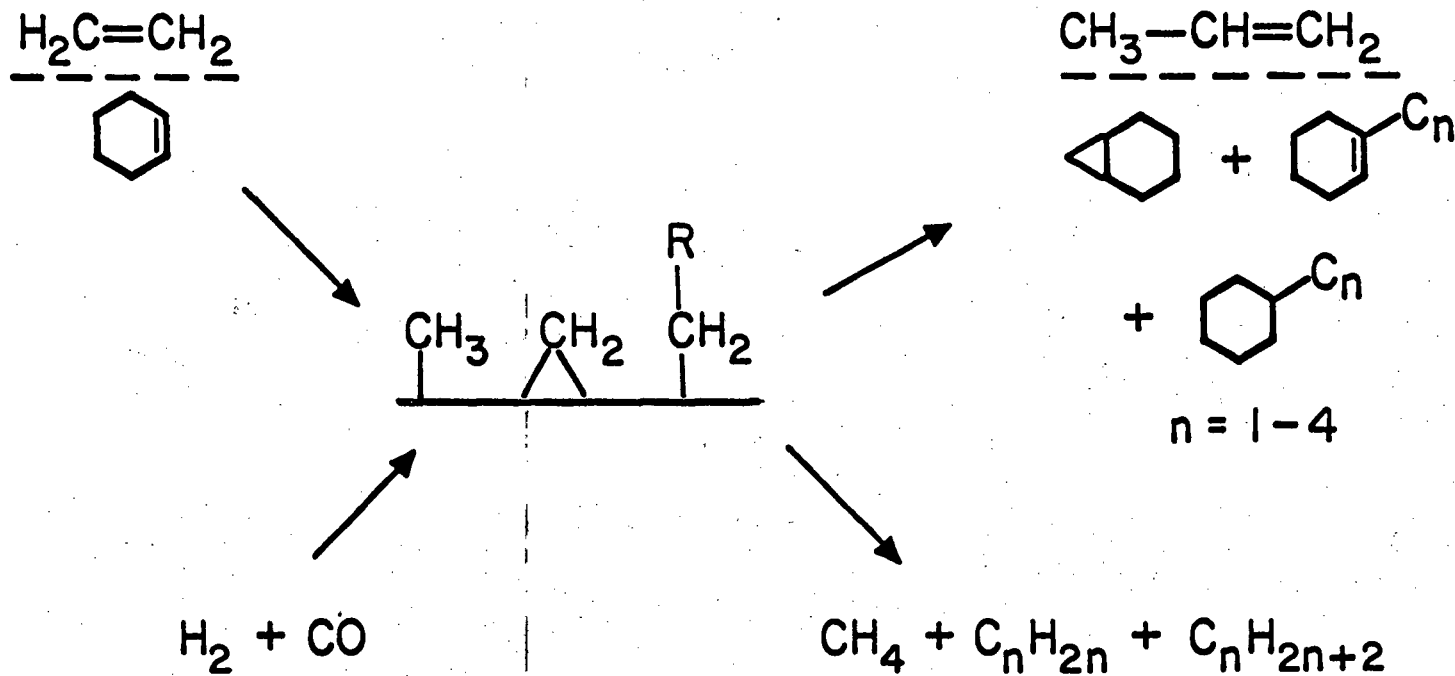


Figure 5

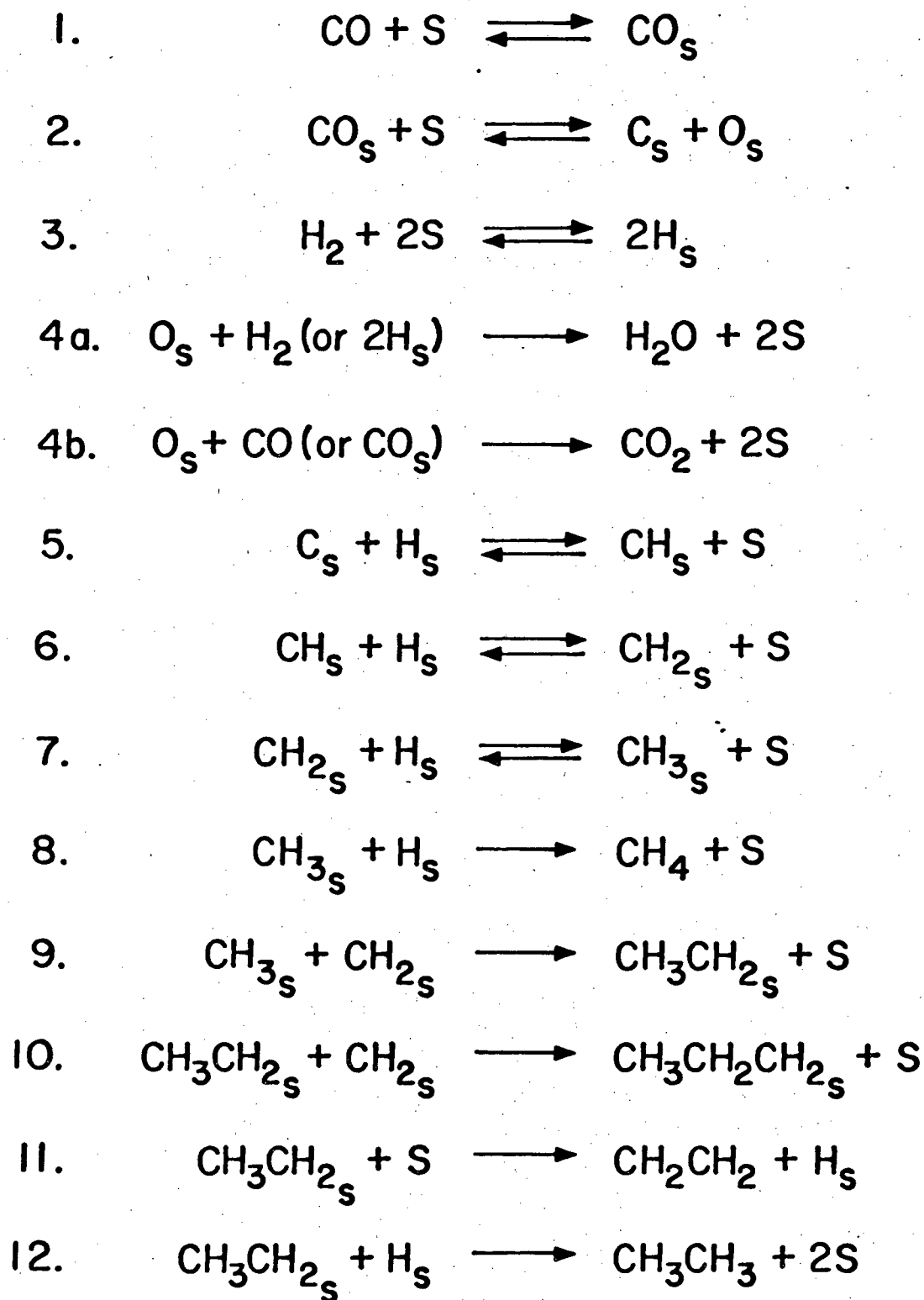
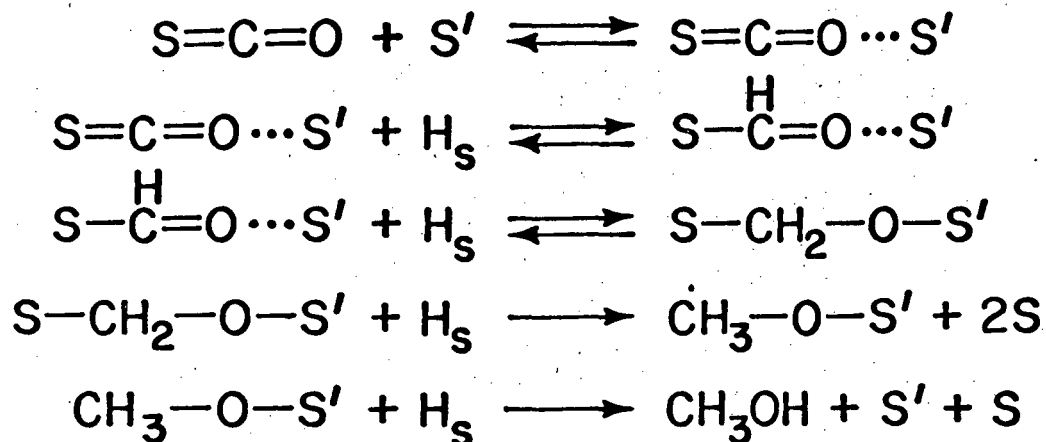
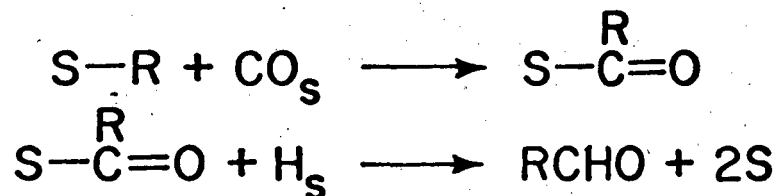


Figure 6

### A. METHANOL



### B. ALDEHYDES



### C. HIGHER ALCOHOLS

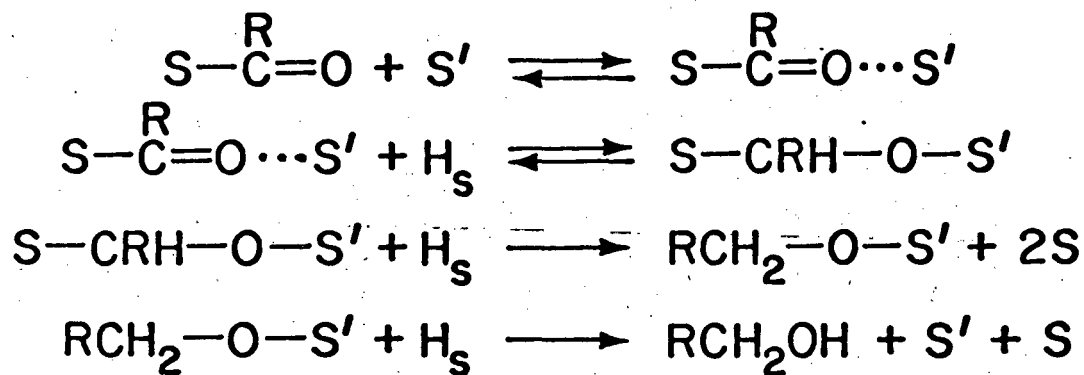


Figure 7

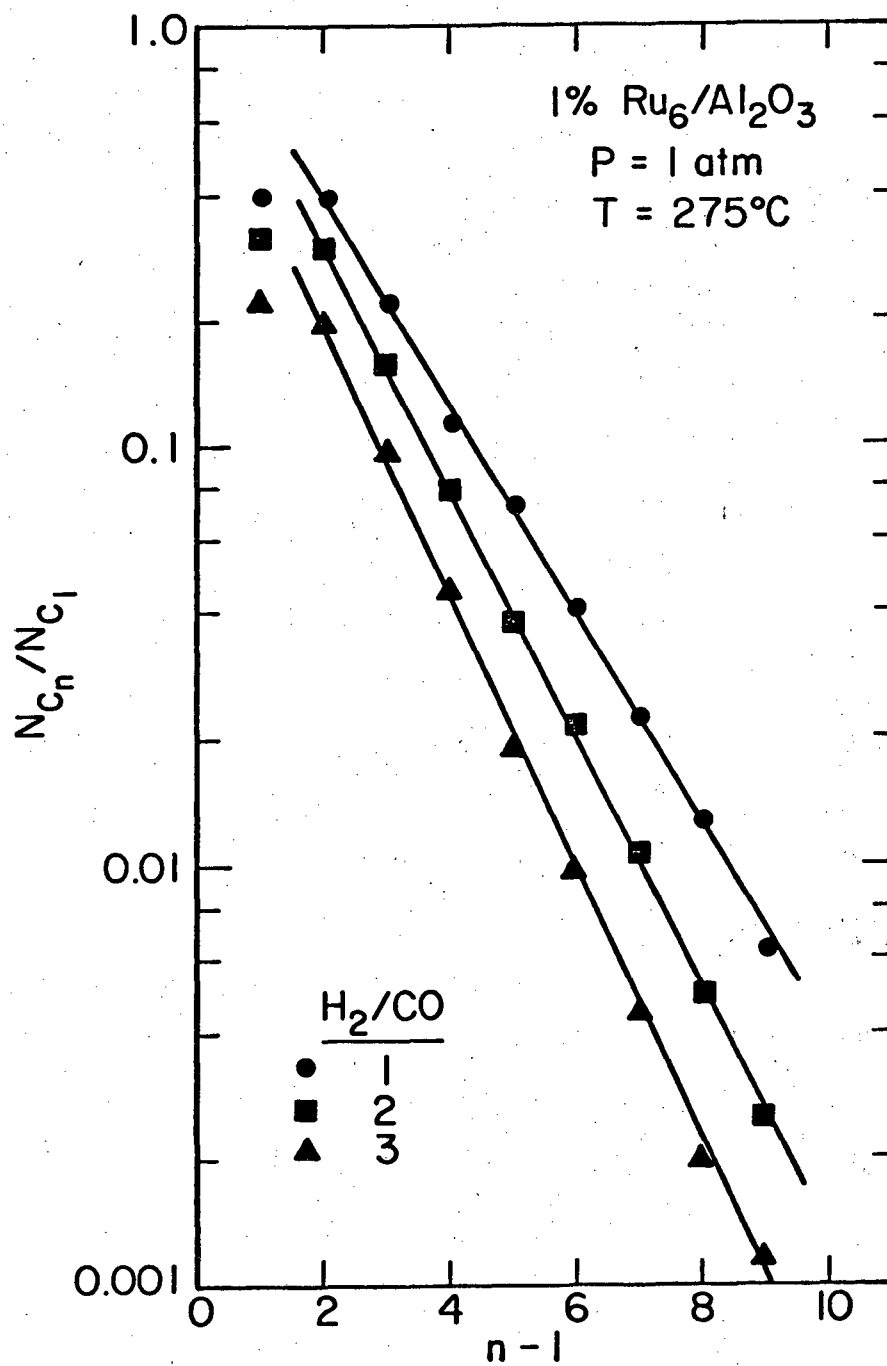


Figure 8

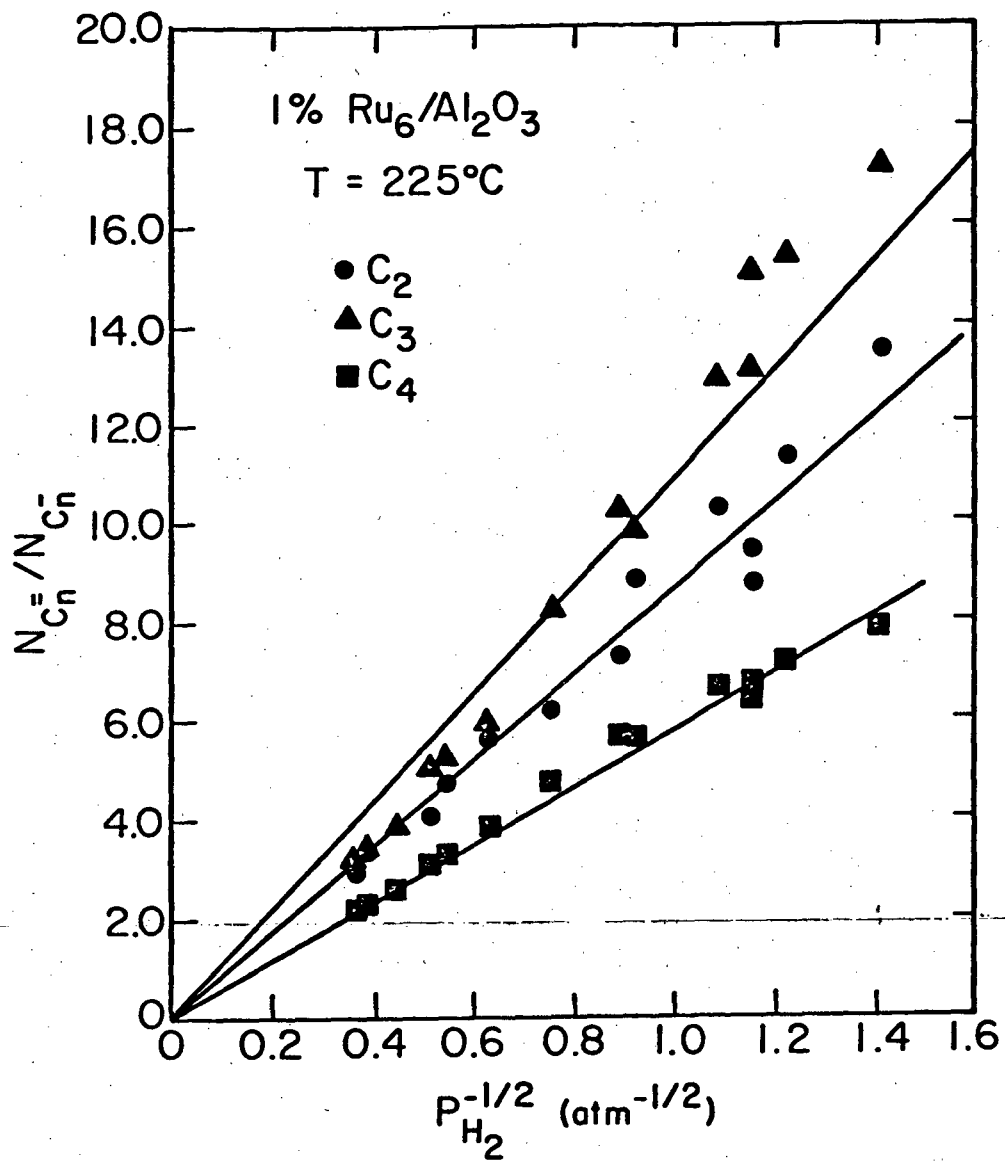


Figure 9



This report was done with support from the Department of Energy. Any conclusions or opinions expressed in this report represent solely those of the author(s) and not necessarily those of The Regents of the University of California, the Lawrence Berkeley Laboratory or the Department of Energy.

Reference to a company or product name does not imply approval or recommendation of the product by the University of California or the U.S. Department of Energy to the exclusion of others that may be suitable.

TECHNICAL INFORMATION DEPARTMENT  
LAWRENCE BERKELEY LABORATORY  
UNIVERSITY OF CALIFORNIA  
BERKELEY, CALIFORNIA 94720